On the microstructure and thermal stability of rapidly quenched Fe–B alloys in the intermediate composition range between the crystalline and amorphous states

M. B. Fernández van Raap and F. H. Sánchez
Departamento de Fisica, Facultad de Ciencias Exactas, Universidad Nacional de La Plata, Casilla de Correos 67, 1900 La Plata, Argentina

Y. D. Zhang
Physics Department, University of Connecticut, 2152 Hillside Road, Storrs, Connecticut 06269

(Received 6 October 1993; accepted 10 April 1995)

The structure and the thermal stability of the $Fe_{0.89}B_{0.11}$ rapidly quenched alloy have been investigated. Transmission Mössbauer measurements were carried out as a function of temperature in the range from 148 K to 513 K. Room temperature x-ray diffraction and transmission and conversion-electron Mössbauer experiments, as well as 4.2 K spin-echo nuclear magnetic resonance measurements, were also performed after some selected thermal treatments for one hour between 523 K and 1273 K. Based on these experiments it is suggested that the alloy is inhomogeneous at nanoscopic scale and consists of a fine dispersion of a defective boride phase with an o–Fe_3B-like short-range order, embedded in an α–Fe matrix. This result gives support to the models which indicate phase separation in the amorphous phase with o–Fe_3B short-range order prevailing in the hypereutectic iron concentration range. This phase was found to be less stable than the undefective one present in the less boron concentrated alloys. The transformation into the equilibrium phases, analyzed with an Arrhenius-type temperature dependence for the increase of the relative fraction of Fe_2B, led to an activation energy $E_a = 1.38 \pm 0.68$ eV/atom.

I. INTRODUCTION

$Fe_{1-x}B_x$ ($0.12 \leq x \leq 0.25$) rapidly quenched alloys have been extensively studied by several methods including the Mössbauer Effect (ME). In order to explain the strange behavior of their physical properties in the vicinity of the eutectic composition, and the different types of crystallization processes, in two steps for $x < 0.17$ and in only one step for $x > 0.17$, an heterogeneous model for the amorphous structure with two iron environments has been proposed[1]: metallic sites with at least one B near neighbor (nn) and whose average metalloid concentration is $x_c = 0.20$, and metallic sites without B nn. Short-range order (SRO) of bct–Fe_3B-type has been proposed for the first class of sites, while from the comparison of NMR and ME studies the existence of both o–Fe_3B and bct–Fe_3B SRO in Fe–B amorphous alloys has been suggested, with a preference for o–Fe_3B SRO in the low boron concentration regime and for bct–Fe_3B in the high boron concentration regime.[2,3] The common feature of these models (and others[4]) is that they are inhomogeneous at a nanoscopic scale, and Fe-like and Fe_3B-like amorphous regions coexist. We suggest here that the SRO that appears in the transition composition range between the crystalline and amorphous state should prevail in the phase separated amorphous system within the hypereutectic composition range.

On the other hand, iron-rich crystalline alloys ($0.01 \leq x \leq 0.09$) had been reported having a different microstructure. Based on the fact that the lattice parameter of α–Fe decreases with increasing B concentration, it was first concluded that the Fe–B crystalline alloys were essentially extended range bcc solid solutions, in which B atoms substituted for Fe atoms in a statistically random way.[5] However, it was later shown that these are heterogeneous systems. These consist of a fine dispersion of minute boride particles or complexes embedded in an α-iron matrix, with SRO identified as o–Fe_3B type.[6] HREM measurements have shown diameters between 5 and 15 Å for these regions.[7] These results together with those obtained from ^{11}B and ^{10}B spin-echo NMR and extended x-ray absorption fine structure at the Fe sites are reviewed in Ref. 7.

Much knowledge has been gained on this system both in the amorphous and crystalline states, but there are only preliminary studies in the intermediate composition range ($0.09 \leq x \leq 0.14$) where the microstructure changes from crystalline to amorphous. This ME research[8] has indicated only that the alloy becomes

more complex as the amorphization composition limit $x \simeq 0.11-0.14$ is approached and that it is not possible to analyze these spectra with simple assumptions like a mixture of boride crystalline phases, being not possible to determine if the system consists of a mixture of α–Fe and other stable or metastable borides or if a small amount of the amorphous phase coexists with the crystalline one. We choose here the $Fe_{0.89}B_{0.11}$ alloy in order to establish the microstructure in this range as well as how crystalline or amorphous formation depends on the composition. Questions as to why, in a fast cooling regime at low boron concentration, the nucleation of Fe_2B is suppressed while o–Fe_3B nucleation is favored are connected with the microstructure of this composition range and will be discussed.

In summary, we report on Mössbauer effect and spin-echo NMR measurements of the rapidly quenched $Fe_{0.89}B_{0.11}$ alloy, in the as-quenched state, after some selected thermal annealings, and also as a function of the measurement temperature between 148 and 513 K. We choose this composition because a possible connection can be established between the microstructure of the crystalline and amorphous alloys. We study the thermal stability of this alloy and compare the results with those obtained from $Fe_{0.91}B_{0.09}$.[9] Finally, we use here a recently developed empirical correlation between isomer shift (δ_{IS}) for ordered stable and metastable Fe–B compounds and local structure parameters (number and type of nn and mean Fe–Fe distance). This correlation may be useful in the analysis of the ME spectra of amorphous alloys as has occurred with the correlation existing between ^{57}Fe hyperfine (hf) field and the number of B nn to an iron atom[1] in these compounds.

II. EXPERIMENTAL

The specimens were prepared by rapid quenching of iron-boron liquid solutions to room temperature using the chill-casting technique.[10] Details of the alloy preparation can be found elsewhere.[5]

The ME experiments were performed using the 14.4 keV resonance of ^{57} Fe with a 6 mCi ^{57}Co*Rh* source. All δ_{IS} are given relative to α–Fe. The measurements were carried out under transmission and electron re-emission (CEMS) geometry in the constant-acceleration mode. The data were accumulated in two halves, 256 channels each, corresponding to the positive and negative accelerations of the transducer. The parabolic deformation of the base line was corrected by a folding procedure, so a unique 256-channel spectrum was used. The velocity scale was calibrated using the six lines of a standard α–Fe absorber with a line width of 0.25 mm s^{-1}.

Spin-echo NMR experiments were made at 4.2 K with zero external magnetic field and for frequencies ranging from 20 to 50 MHz. The pulsed NMR apparatus and data-taking procedure have been described in detail elsewhere.[11]

ME temperature measurements were performed with an oven under a vacuum of better than 10^{-3} Torr. Thermal annealings were carried out using a conventional electrical oven under a low pressure argon atmosphere.

Finally, the ME spectra were fitted with Lorentzian curves with respect to the of-resonance background. In the fitting procedure the relations L_1/L_2 and L_1/L_3 were allowed to vary, taking into account the effective thickness of the absorber. This was done in a consistent way with the relative intensity of each subspectrum.[12] Analyses with a combination of Lorentzian lines and a distribution of hyperfine (hf) fields were also tried. This approach led to essentially the same information as the first one, but it was set aside since it resulted in a poorer fitting quality.

The as-quenched and some of the thermal-treated samples were characterized by Kα(Co) x-ray diffraction. The lines of the as-quenched alloy could be indexed using a bcc structure with a lattice parameter slightly lower than that of α–Fe, consistent with the reported decrease of the lattice constant with the boron concentration for $0.01 \leq x \leq 0.12$.[5,7]

III. RESULTS AND DISCUSSION

A. The as-quenched alloy

The spectrum of the original alloy (see Fig. 1) and those taken after annealing for an hour at temperatures between 623 and 716 K were best fitted with five magnetic interactions, characterized by hyperfine parameters listed in Table I. The magnetic interaction corresponding to site 0 is identical to that of α–Fe, and, hence, is associated with ^{57}Fe probes in regular bcc sites and surrounded by eight nearest-neighbor Fe atoms. The remaining interactions are characterized by linewidths larger than 0.25 mm/s (the experimental resolution), suggesting disorder. The more intense ones (sites 4 and 2) are similar to those of o–Fe_3B, although the relative intensities do not satisfy the ratio 2 : 1 observed in this compound (see Table II). Interaction 1 is the same as one of those observed in t–Fe_3B, while interaction 3 does not correspond to any of those reported for known borides. However, it must be mentioned that a direct identification of the borides present in the as-quenched material may not be ambiguously made only on the basis of the hyperfine interactions when a mixture of phases is present. This limitation arises from the fact that there are sites in different borides with similar hf parameters (see Table II). In Fig. 1 the CEMS spectrum of the as-quenched alloy (1000–3000 Å from the surface) is also shown. Only three hf interactions were needed to describe the data which correspond to a mixture of only

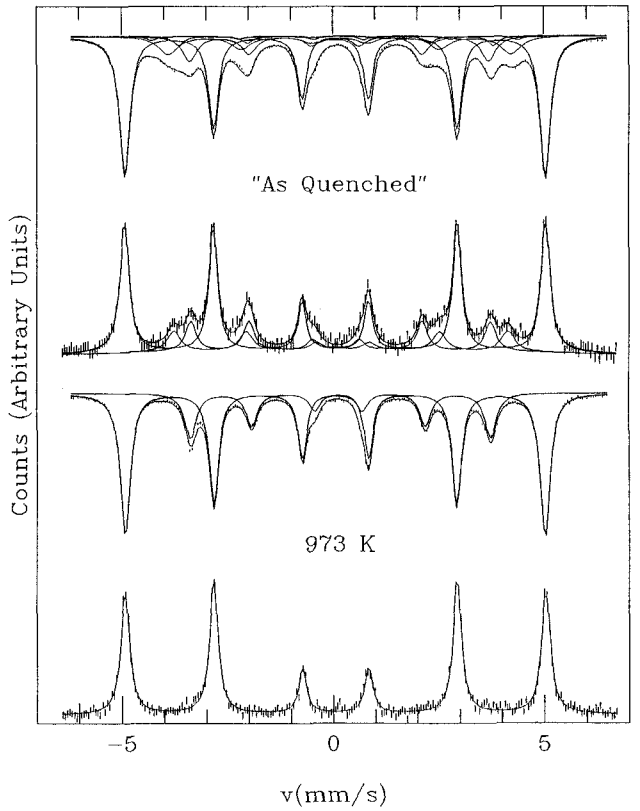

FIG. 1. Room temperature Mössbauer spectra in transmission and electron re-emission geometry of the as-quenched $Fe_{0.89}$ $B_{0.11}$ alloy and after thermal annealing at 973 K for 1 h.

o–Fe_3B and α–Fe with relative intensities consistent with the alloy nominal composition.

From the ME spectra the bulk boride phases involve about 37% of the total Fe atoms. However, only 3% of the XRD reflections do not correspond to α–Fe, and those contributions are almost completely concentrated around $\Theta = 25.25°$ ($d = 2.098$ Å). These contributions may correspond to the reflections (002) of Fe_2B, (321), and (231) of t–Fe_3B and/or (220) of o–Fe_3B,[13] and therefore do not allow a conclusive identification of the boride phases. Furthermore, as XRD is sensitive only to well-developed phases, the small contributions of the boride phases to the XRD spectrum indicate that these phases are highly disperse in the form of small particles,

TABLE I. Room-temperature hyperfine fields (H), isomer shifts (δ_{IS}), and quadrupole shifts (ϵ) associated with the five sites found for the ^{57}Fe probes in the as-quenched $Fe_{0.89}B_{0.11}$ samples.

Site	H (kOe)	δ_{IS} (mm/s)	ϵ (mm/s)
0	331.3 ± 0.2	0.001 ± 0.001	0.002 ± 0.001
1	288.0 ± 1.6	0.048 ± 0.019	0.056 ± 0.023
2	270.3 ± 0.7	0.144 ± 0.007	0.023 ± 0.005
3	249.1 ± 0.6	0.057 ± 0.006	0.022 ± 0.006
4	235.9 ± 0.4	0.067 ± 0.003	−0.043 ± 0.003

in agreement with previous observations of alloys less concentrated in boron.[6]

These results are consistent with that obtained with the spin-echo NMR technique, which is shown in Fig. 2. This spectrum indicates resonance peaks at the frequencies of 35 MHz and 40 MHz superimposed to a broad distribution centered about 30 MHz. The two peaks can be assigned to resonances of ^{57}Fe in o–Fe_3B and correspond to the most populated fields in the ME spectrum (see Table III). A contribution at 39 MHz, as that measured[7] for ^{11}B in the as-quenched more boron diluted alloys, can also be inferred from the form of the spectrum. It must be noticed that there is no resonance peak at 41.3 MHz, indicating absence of Fe_2B. The distribution is a surprising result because ^{11}B and ^{57}Fe resonances have never been reported at frequencies lower than 35 MHz for this system, except for boron in the compound FeB (13.4 MHz).[3,14] One possible explanation for this distribution is that the boride phase could be defective, having at the same time vacancies at B sites, interstitial B, and/or the substitution of Fe by B in the o–Fe_3B structure. As the boron field is mainly determined by the iron neighbors, each with moment μ_i

$$H = A \sum_i \mu_i$$

(where A is the so-called hyperfine constant), the presence of B as interstitial or substituting the Fe would produce a reduction of the magnetic moment of the iron atoms, and/or a diminution in the number of magnetic moments, respectively, thus reducing the transferred hf field. This, in turn, would produce a ^{11}B hf field distribution at lower frequencies.

In an attempt to separate the ^{11}B and ^{57}Fe contributions to the NMR spectrum, we have determined, in terms of NMR frequency units, the discrete ^{57}Fe hf field distribution obtained from the ME spectrum. It can be seen in Fig. 2 that this distribution is qualitatively similar to the NMR spectrum obtained after subtracting the distribution about 30 MHz. The noticeable difference between the intensities of the ^{11}B and the ^{57}Fe distributions arises from the different sensitivity factors.

In order to gain further insight concerning the nature of the boride phases, the temperature dependence of the hf field was investigated, for temperatures in the range from 148 K to 513 K. Measurements at higher temperatures were not possible because the boride phase undergoes a transformation during the time required for data acquisition (typically, several hours). Figure 3 shows this dependence for the five hf fields along with those from α–Fe, o–Fe_3B, and Fe_2B. As can be seen, the four boride hf fields follow, within the experimental error, the same temperature dependence, although this is different from that of Fe_2B and α–Fe. It is important to point out here that the values and intensities of the

TABLE II. Room-temperature ^{57}Fe hyperfine fields (H), isomer shifts (δ_{IS}), quadrupole shifts (ϵ), and relative populations (F) for the nonequivalent iron sites in the known iron-borides and in bcc and fcc Fe.

Boride	Site	H (kOe)	δ_{IS} (mm/s)	ϵ (mm/s)	F	Reference
FeB	1	118	0.26	0.06	1.00	26
Fe_2B	1	232	0.12	0.02	0.50	
	2	242	0.12	0.04	0.50	16
	Average	237	0.12	0.03	1.00	
t–Fe_3B	1	288	0.06	0.04	0.33	
	2	265	0.03	0.09	0.33	27
	3	225	0.11	−0.06	0.33	
o–Fe_3B	1	264	0.13	0.11	0.33	
	2	235	0.07	0.02	0.67	28
	1	267	0.19	0.02	0.33	
	2	236	0.09	0.07	0.67	6, 29
$Fe_{23}B_6$	1	288	...	...	0.35	
	2	238	...	...	0.53	
	3	...	...	...	0.09	30
	4	...	...	...	0.04	
α–Fe	1	330	0.00	0.00	1.00	31
γ–Fe	1	...	−0.10	...	1.00	32

four magnetic interactions cannot be reproduced by any mixture of known borides, as for example o–Fe_3B and t–Fe_3B (which have Curie temperatures of about 880 K[6] and 800 K,[15] respectively, in agreement with the hf field temperature dependence shown in Fig. 3).

These results allow us to discard the presence of amorphous phases as they have magnetic ordering temperatures between 552 and 760 K[15] as well as the presence of Fe_2B. Also they strongly suggest that sites 1, 2, 3, and 4 belong to a single boride phase.

Approximately, the ME subspectra of the five ^{57}Fe sites (0 to 4) have constant relative intensities in the whole temperature range, indicating similar recoil free fractions for probes at the different sites. This is also consistent with the interpretation that these four sites belong to a single boride phase.

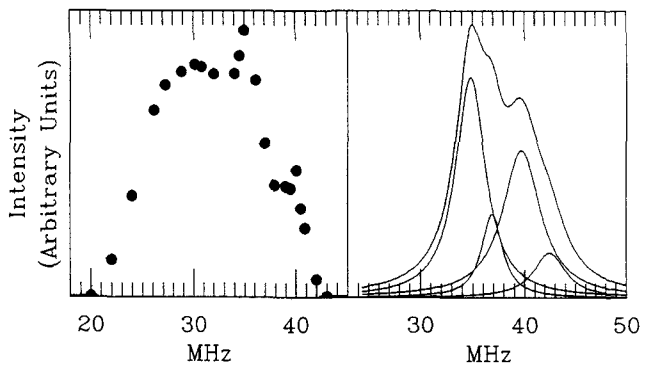

FIG. 2. Spin-echo NMR intensity of the as-quenched $Fe_{0.89}B_{0.11}$ alloy (left) and ^{57}Fe hf field distribution in NMR frequency units (using the conversion coefficient $\gamma = 0.1374$ MHz/kOe), obtained from the ME spectrum shown in Fig. 1 (right).

The δ_{IS} values of the five sites are displayed as a function of temperature in Fig. 4. Their rate of linear decrease with temperature agrees very well with the second order Doppler effect value of $-7.29\ 10^{-4}$ mm/sK expected for the 14.4 keV transition of ^{57}Fe, confirming that our description of the ME spectra with five sextets is consistent.

From the composition x and the fraction f_0 of Fe atoms in α–Fe sites, the stoichiometry ζ of the boride $Fe_\zeta B$ can be calculated by means of

$$\zeta = \frac{1 - x}{x}(1 - f_0)$$

The value of ζ was calculated from the spectra taken after thermal annealing at temperatures from 523 K to 1273 K. Figure 5 shows that ζ decreases from a value close to 3 to about 2 in the annealing temperature range of 716–873 K, reflecting the transformation of the original boride phase into Fe_2B which will be discussed later.

TABLE III. ^{11}B spin-echo NMR hyperfine fields in the known crystalline iron-borides and in the amorphous (a–$Fe_{1-x}B_x$) alloys at 4.2 K.

Boride	H_B (MHz)	Reference
FeB	13.4	3, 14
Fe_2B	41.0	3, 14
t–Fe_3B	34.4	3
O–Fe_3B	36.2	3
	39.0	7
$Fe_3B_{1-x}C_x$	36.3	17
$Fe_{23}B_6$	38.0	13
a–$Fe_{1-x}B_x$ ($0.14 \leq x$ 0.22)	38.5–35.9	25

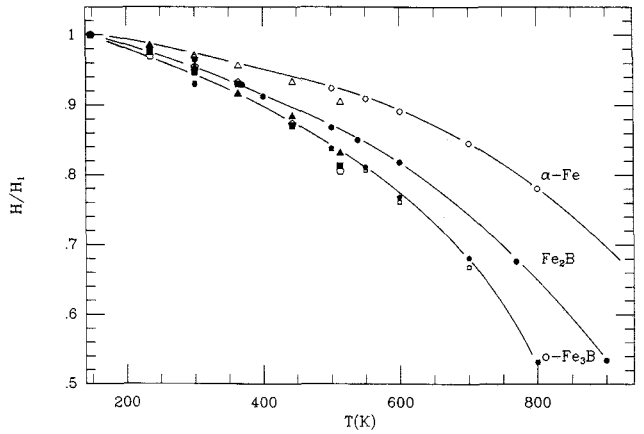

FIG. 3. ^{57}Fe hf field values H/H_1 in reduced units with respect to the lower temperature of measurement (148 K) versus absolute temperature T in K for the five sites in the as-quenched $Fe_{0.89}B_{0.11}$ alloy (big dots), in bcc–Fe and in sites 1 and 2 in o–Fe_3B-like complexes, for $Fe_{0.95}B_{0.05}$ and $Fe_{0.91}B_{0.09}$ alloys (Ref. 7), and in Fe_2B (Refs. 16 and 33).

It is well known that in boride compounds the ^{57}Fe hf field H_i mainly depends on the metalloid neighborhood of iron site i. Le Caër *et al.*[1] have restricted the correlation to the number n_B^i of B nearest neighbors, neglecting the Fe–B distances. They proposed the following relationship, valid at room temperature,

$$H(\text{kOe}) = 345 - 31n_B^i \qquad (1)$$

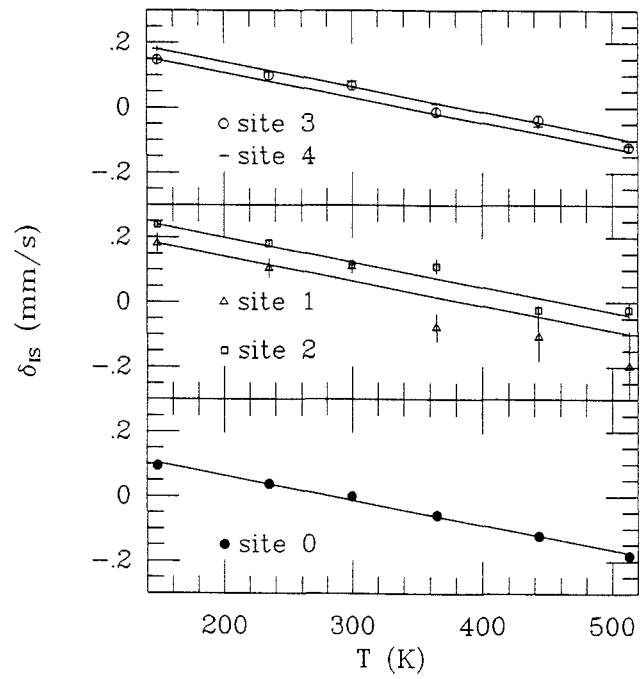

FIG. 4. Temperature dependence of the isomer shift for the five sites in the as-quenched $Fe_{0.89}B_{0.11}$ alloy relative to α–FeRT. The solid lines correspond to the slope that fit best the site 0 (^{57}Fe in α–Fe) isomer shift evolution.

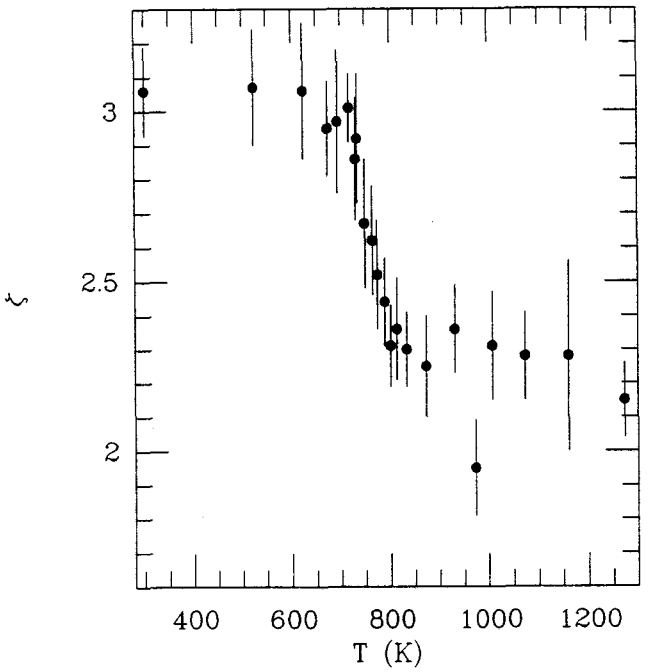

FIG. 5. Calculated stoichiometry ζ of the boride phase $Fe_\zeta B$ versus annealing temperature for thermal treatments of 1 h. The value obtained from the nontreated sample is included.

Using this correlation we have calculated n_B^i for each iron site and from the relative ME subspectra intensities, the average number $\overline{n}_B$. Then the number of iron-boron pairs has been estimated from $\overline{Z}_{Fe-B} = \zeta\overline{n}_B$. These values were calculated in the whole range of annealing temperatures and it was found that $\overline{n}_B$ increases from nearly 3 to 4 while $\overline{Z}_{Fe-B}$ decreases from approximately 9 to 7. It is worth mentioning that $\overline{n}_B$ and $\overline{Z}_{Fe-B}$ have values of 3 and 9, respectively, for both o–Fe_3B and t–Fe_3B, and of 4 and 6 for Fe_2B, therefore reinforcing the identification of the original boride phase as a sort of Fe_3B, as well as its evolution toward Fe_2B. Since we do not expect the existence of B–B pairs, the quantity $\overline{Z}_{Fe-B}$ coincides with the coordination number of the B atoms. Therefore we may conclude that the original system contains only one boride phase described by the formula Fe_3B. Under the melt-spinning kinetic conditions the lower free energy of the alloy corresponds to the mixture of o–Fe_3B and α–Fe, excluding other possibilities like mixtures of o–Fe_3B, Fe_2B, and α–Fe or mixtures of o–Fe_3B, t–Fe_3B, and α–Fe. Based on this result and others previously reported,[6,8] a thermodynamic model, which takes into account the extremely high dispersion state of the boride phase and the high degree of coherence between o–Fe_3B-like complexes and the α–Fe, has been developed.[19] Within this model the absence of Fe_2B nucleation is understood as due to the high free energy of the α–Fe/Fe_2B interface ($\sigma \cong$

50 kJ/g atom) as compared with the α–Fe/o–Fe_3B interface free energy ($\sigma \cong 4.5$ kJ/g atom).

B. Thermal evolution

The evolution of the fractions f_i of the ^{57}Fe probes at different sites with the annealing temperature is shown in Fig. 6. It shows that the boride transforms with little or no iron segregation between 623 and 716 K, since the intensity associated with site 0 is nearly constant while the other ones change. The ME spectra taken after annealing at 716 K and that recorded for the as-quenched $Fe_{0.91}B_{0.09}$ alloy are displayed together in Fig. 7 in order to show the similarity between them. The latter was fitted with the hf parameters of o–Fe_3B and α–Fe. After the thermal treatment at 733 K the fraction f_0 increases and sites 1 and 3 disappear. The increment in fraction f_0 is connected with the decomposition of the boride phase into Fe_2B and α–Fe. In this temperature interval, in order to achieve a good description of the ME spectra it was needed to split interaction 4 into two contributions 4 and 4′ of nearly equal hf fields, isomer shifts, and intensities, but quadrupole shifts of different sign. This situation is typical of magnetic anisotropy effects as in Fe_2B[16] and agrees with the evolution of part of the system toward this phase. It is interesting to note that the magnetic anisotropy is not present in the ME spectrum taken after annealing at 1273 K. As this temperature is greater than the Curie one of Fe_2B, when the sample was cooled down to room temperature the magnetization was induced in the direction for which the iron atoms are magnetically equivalent in Fe_2B.

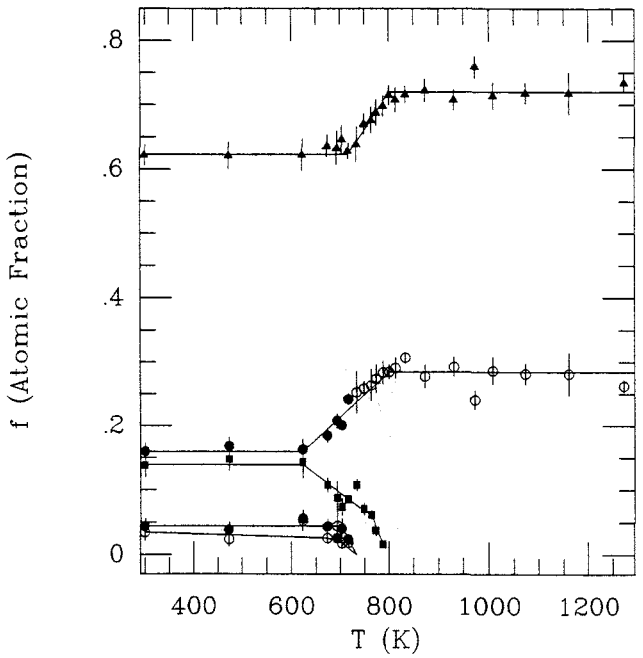

FIG. 6. From top to bottom: evolution of the ^{57}Fe atomic fractions at sites 0, 4, 2, 3, and 1 with annealing for 1 hour. For site 4 open dots are used to indicate average fractions when hf field splitting due to magnetic anisotropic effects is present. Values obtained from the nontreated sample are included.

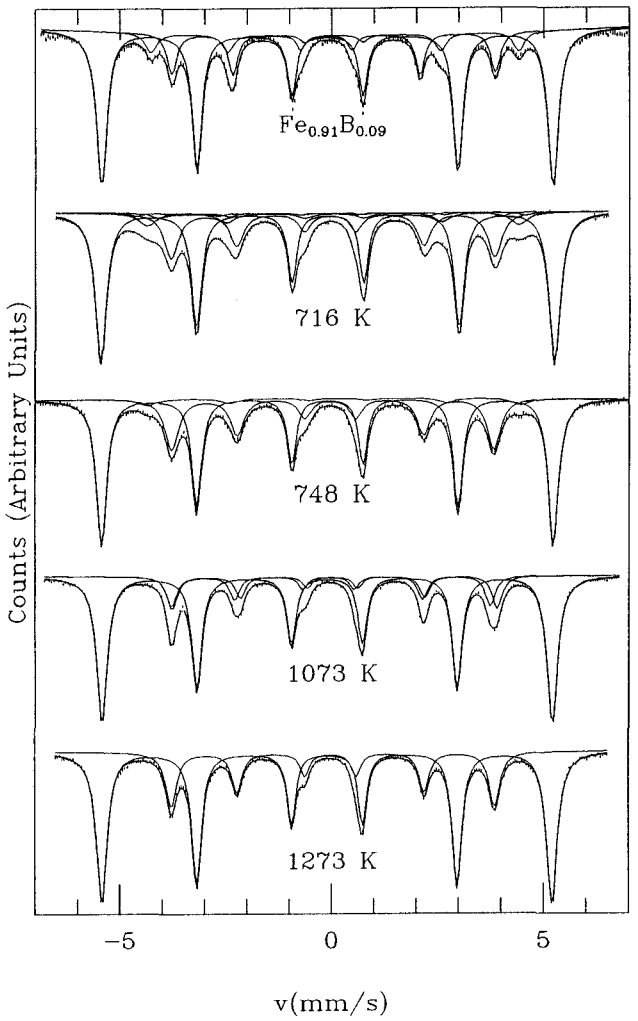

FIG. 7. From top to bottom: room temperature Mössbauer spectra of the as-quenched $Fe_{0.91}B_{0.09}$ alloy and of $Fe_{0.89}B_{0.11}$ annealed at 716, 748, 1073, and 1273 K.

It is known that in the transformation from o–Fe_3B to Fe_2B + α–Fe, the contribution to the ME spectra of the interaction with the hf field of 234 kOe remains constant,[9] while the δ_{IS} changes from 0.07 to 0.12 mm/s. The evolution of δ_{IS}, and of the average quadrupole shift ϵ for the site 4 are shown in Fig. 8, while the average boride linewidth $\overline{\Gamma}_B$ for the boride sites and the linewidth for α–Fe are shown in Fig. 9. These results are consistent with the transformation of the Fe_3B-type original phase toward Fe_2B and reveal the simultaneous ordering of the system.

Spin-echo NMR experiments were performed after thermal treatments at 716 and 773 K. Figure 10 shows the NMR spectra together with the distribution of ^{57}Fe hf fields (obtained from the ME results). These spectra, taken in the frequency range from 30 to 50 MHz, show

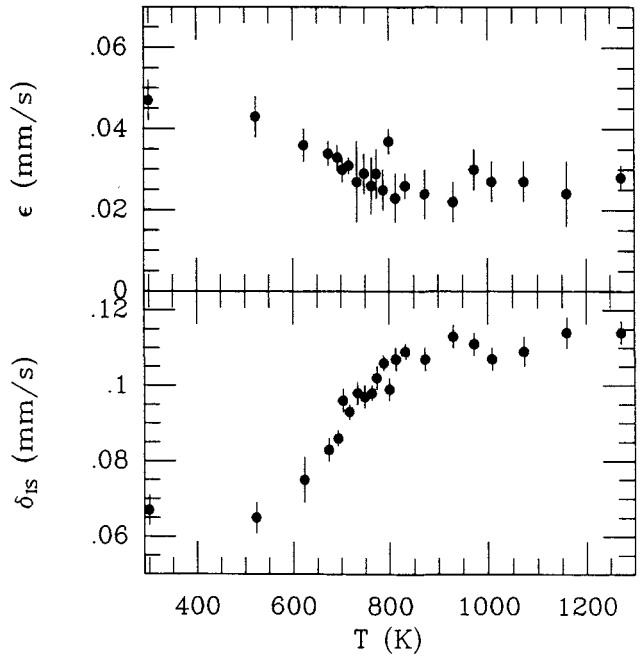

FIG. 8. Evolution of the measured isomer shift and quadrupole shift for site 4 with annealing temperature.

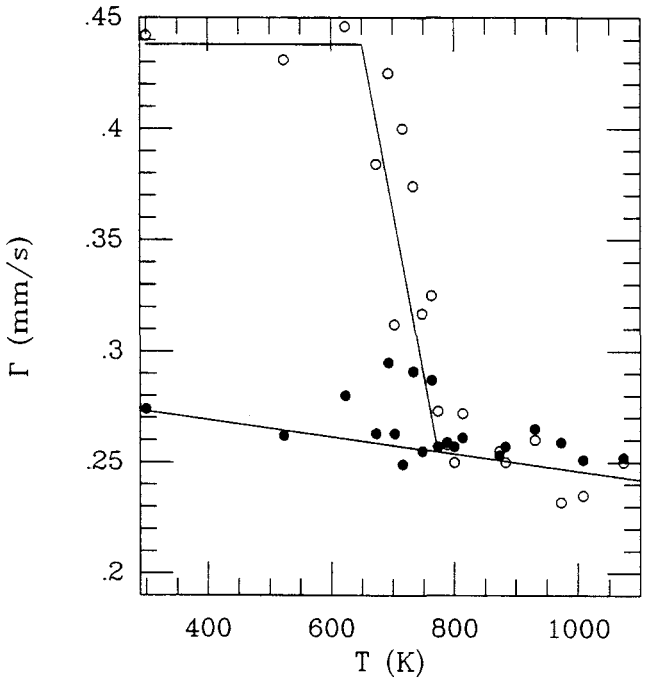

FIG. 9. Average boride linewidth (○) and α–Fe linewidth (●) versus annealing temperature.

resonances at 46.7 MHz (from α–Fe not shown in the picture), 40.4, and 36.2 MHz. These last two peaks are wider than those expected from crystalline sites corresponding to the superposition of several contributions. The form and asymmetry of the peaks suggest that they are the result of the contributions of ^{57}Fe

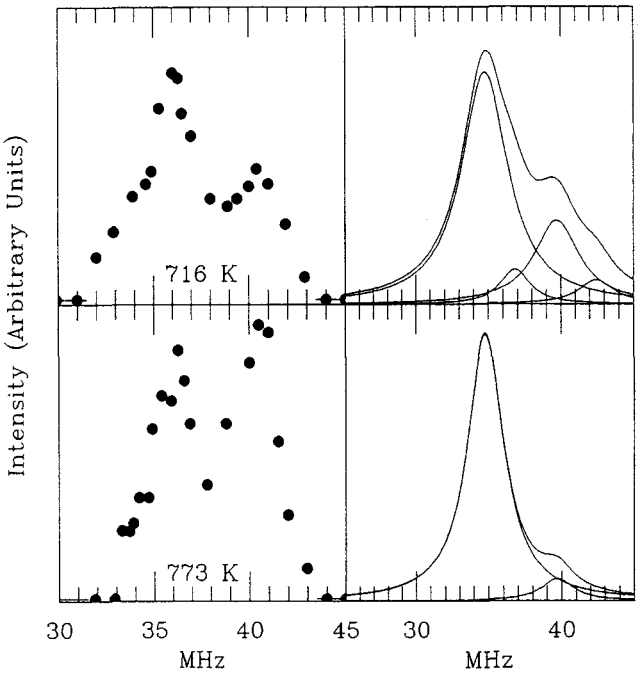

FIG. 10. Spin-echo NMR intensity of the rapidly quenched $Fe_{0.89}B_{0.11}$ alloy annealed for 1 h at 716 and 773 K (left) and ^{57}Fe hf field distribution obtained from the ME spectra, in frequency units using the conversion coefficient $\gamma = 0.1374$ MHz/kOe (right).

resonances at 35 and 40 MHz, and ^{11}B resonances at 39, 41, and 36.2 MHz. The resonance at 36.2 MHz corresponds to ^{11}B in a more ordered o–Fe_3B structure. This frequency value has been obtained in o–Fe_3B stabilized with other elements as Co,[18] Ni,[29] or C[17] and it is different from that measured in the as-quenched $Fe_{1-x}B_x$ alloys at 39 MHz.[7] After the thermal treatment at 773 K, the NMR spectrum shows appreciable differences. The intensity of the second peak increases due to the contribution of the ^{11}B resonance in Fe_2B (at 41 MHz), as can be seen by comparison with the ^{57}Fe hf field distribution.

Our results show that the evolution of the system toward the equilibrium state involves two steps: evolution of the system to a more ordered o–Fe_3B with little or no iron segregation (until thermal annealing at 716 K) followed by decomposition into the equilibrium phases. Since in the first transformation the superposition of the two processes cannot be excluded, we use the higher annealing temperature range (716–800 K) to determine the activation energy which characterizes the transformation. In order to obtain the normalized fraction of Fe_2B formed during annealing of one hour at temperature T we follow the evolution of the fraction f_0 of the ^{57}Fe probes at α–Fe sites. This fraction is the one subject to the smallest relative errors and its increment proceeds unmistakable from Fe_2B formation. Therefore, the relative fraction of iron atoms in Fe_2B is

calculated from

$$\Omega(T) = \frac{f_0(T) - f_0(0)}{f_0(\infty) - f_0(0)}$$

where $f_0(0)$ is the initial fraction of iron probes in α–Fe and $f_0(\infty)$ is the one corresponding to the complete transformation. Assuming a process driven by nucleation and growth, the activation energy can be obtained from the plot of $\ln\{\ln(1/1 - \Omega)\}$ vs $1/T$ shown in Fig. 11 (from the data in Fig. 6 corresponding to annealing temperatures ranging from 716 to 800 K). The obtained value, $E_a = 1.38 \pm 0.68$ eV/atom, is much lower than that observed for the alloy with 9% of B ($E_a = 3.5 \pm 0.07$ eV/at), system which needed more than 60 h at 773 K to become completely transformed. These results indicate a lower stability in the present case. The lower value of E_a might be due to the defective nature of the boride phase, a situation which should enhance the diffusion rate. Furthermore, the different activation energies in both alloys (9 and 11%) may correspond to the existence of slightly different microstructures. In the first case, in order to grow a Fe_2B particle from several o–Fe_3B complexes, the boron atoms have to be unbound from the boride and then interstitially created in bcc–Fe, since the o–Fe_3B complexes are mostly isolated from each other. These two processes demand energy expenditure. In the second case, due to the higher boron concentration, the boride regions must be interconnected to a larger extent and, so, different diffusion paths may coexist across α–Fe and/or boride regions, modifying the effective activation energy. The activation energy reported for diffusion of B in Fe_2B ranges from 1.10 eV/at to 1.64 eV/atom.[20]

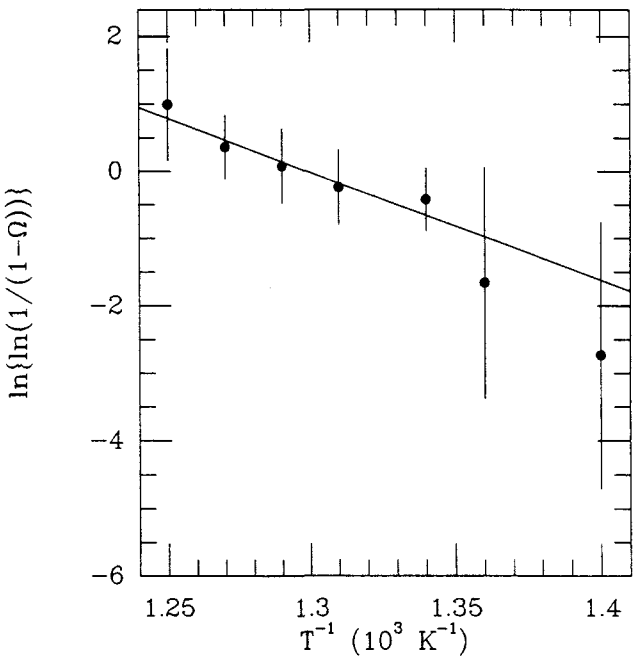

FIG. 11. A plot of $\ln\{\ln[1/1 - \Omega]\}$ as a function of the reciprocal temperature for annealings of 1 h at temperatures from 716 K to 800 K. The slope of the straight line fitted to the experimental points corresponds to an activation energy of 1.38 ± 0.68 eV/atom.

From the comparison of the ME spectra of the sample annealed at 973 K in transmission and electron reemission geometry, it is clear that the boron atom is the diffuser (see Fig. 1). The former shows the hf interactions characteristic of α–Fe and Fe_2B, while the latter shows only the one corresponding to α–Fe, indicating the absence of the boride phase at the surface of the material (typically 1000–3000 Å).

C. Empirical correlation for the isomer shift

As the theoretical understanding of the factors that determine the value of δ_{IS} in alloys is still far from being clear, simple empirical correlations are always useful. We have found that the experimental δ_{IS} values, measured at the seven sites of the Fe–B compounds, as well as those obtained from α–Fe and γ–Fe, may be reproduced (see Table IV) by the following formula:

$$\delta_{IS} = 0.02981 n_B + (\overline{d}_{Fe}(\text{Å}) - 2.643)\frac{n_{Fe}}{12.56} \quad \text{in (mm/s)}$$

where $\overline{d}_{Fe}$ is a mean radius of the first Fe coordination shell (including all iron atoms within a sphere of 3 Å radius), and n_B and n_{Fe} are the numbers of boron and iron neighbors. The constants 0.02981, 2.643, and 12.56 which appear in the last equation have been determined by the least squares procedure using the Marquardt–Levenberg algorithm, and have standard deviations of 1.486 10^{-3}, 5.346 10^{-3}, and 7.874 10^{-1}, respectively.

The most striking feature of this formula is that it depends on the Fe–Fe mean distances but not on the Fe–B mean distances. This is probably due to the more metallic Fe–Fe interaction as compared to the B–Fe one. In the last case, the bonds are more covalent and the electrons are more localized, so that small distance variations would produce nearly the same charge distribution density, and then no effect on the δ_{IS}.

From the first term, it is shown that δ_{IS} increases when increasing the number of B nn. This behavior is expected from experimental studies as well as from semiempirical approaches for other systems like substitutional and ordered alloys. As Ingalls *et al.*[21] have pointed out, the variation in ^{57}Fe δ_{IS} is in many systems approximately additive with the number of nn of a given class. However, these systems are different from the compounds considered here, sometimes called interstitial compounds, and a second term which entails a

TABLE IV. Calculated (δ_{IS}^{Cal}) and experimental (δ_{IS}^{Exp}) isomer shifts for crystalline iron-boron compounds, α–Fe, γ–Fe, and amorphous $Fe_{1-x}B_x$ alloys with $x = 0.20$ and 0.17 (Ref. 24). n_B, n_{Fe}, and $\overline{d}_{Fe}$ are the number of boron and iron neighbors to the iron site, and the average Fe–Fe distance, respectively.

Boride	Site	n_B	n_{Fe}	$\overline{d}_{Fe}$ (Å)	δ_{IS}^{Exp} (mm/s)	δ_{IS}^{Cal} (mm/s)
FeB	1	6	10	2.75	0.26	0.264
Fe_2B	1	4	11	2.63	0.12	0.108
t–Fe_3B	1	2	12	2.638	0.06	0.055
	2	4	10	2.635	0.11	0.113
	3	3	10	2.575	0.03	0.035
o–Fe_3B	1	3	12	2.678	0.13	0.123
	2	3	11	2.628	0.07	0.076
α–Fe	1	...	14	2.647	0.00	0.004
γ–Fe	1	...	12	2.537	−0.10	−0.101
$x = 0.20$	...	2.15	12.4	2.57	0.053	0.064
$x = 0.17$	...	1.41	10.7	2.56	0.042	0.042

volume dependence is needed to reproduce the measured shifts. The volume dependence of the ^{57}Fe isomer shift, $\partial\delta_{IS}/\partial \ln\Omega = 1.33 \pm 0.008$ mm/s at 300 K, has been established by Ingalls[22] from a simple extrapolation of pressure experiments carried out on metallic iron. Deviations from this volume dependence were ascribed to changes in the number of d and s iron valence electrons, n_d and n_s. Ingalls' expression leads, for a typical volume of $\Omega = 11.7$ Å^3, to $\partial\delta_{IS}/\partial\overline{d}_{Fe} = 1.41$ mm/s Å. This value is in good agreement with that obtained from our correlation $\partial\delta_{IS}/\partial\overline{d}_{Fe} = n_{Fe}/12.56 \simeq 1.00$ mm/s Å (see in Table IV that n_{Fe} varies from 10 to 14 only), and specially for the one expected for α–Fe (1.11 mm/s Å). Further details on the correlation are described in Ref. 23.

Using the n_B^i values calculated in Sec. A, we have estimated the values of $\overline{d}_{Fe}$ for the measured δ_{IS} varying n_{Fe} between 10 and 12 (as expected in the iron borides). The values obtained are close to those listed in Table IV, indicating that the measured δ_{IS} are also consistent with the microstructure proposed.

It is worth noticing that this correlation can also be extended for δ_{IS} in the amorphous alloys, but only the first term must be taken into account because in amorphous alloys the atoms of all the composing elements can freely choose their own volume. We make this for $x = 0.20$ and $x = 0.17$ for which structural data are available.[24] It can be seen that in this case also a good agreement is achieved.

IV. CONCLUSIONS

From the ME, NMR, and x-ray diffraction studies of the rapidly quenched $Fe_{0.89}B_{0.11}$ alloy we conclude that the microstructure proposed[6] for $Fe_{1-x}B_x$ ($0.01 \leq x \leq 0.09$) remains valid. That is, the alloy is fundamentally a dispersion of o–Fe_3B in α–Fe. However, in the present case the O–Fe_3B phase became defective. These results give support to studies that suggest a SRO of o–Fe_3B-type for the $Fe_{0.86}B_{0.14}$ and nearby composition amorphous alloys.

The thermal evolution indicates that this alloy is less stable (the transformation began at a rather low temperature) than the less boron concentrated alloys. Evolution toward the equilibrium state includes transformation into a more ordered o–Fe_3B followed by the decomposition into the equilibrium phases. An activation energy of 1.38 ± 0.68 eV/atom was established for the overall decomposition into Fe_2B and α–Fe.

ACKNOWLEDGMENTS

We wish to acknowledge R. Hasegawa who kindly provided the samples for these studies and Bibiana Arcondo who performed the x-ray diffraction characterization. This work was supported in part by the Consejo Nacional de Investigaciones Cientificas y Tecnológicas (CONICET), of the República Argentina.

REFERENCES

1. J. M. Dubois and G. Le Caër, Nucl. Instrum. Methods. **199**, 307 (1982).
2. Y. D. Zhang, J. I. Budnick, J. C. Ford, and W. A. Hines, unpublished.
3. V. S. Pokatilov, Sov. Phys. Dokl. **29** (3), 234 (1984).
4. P. H. Gaskell, J. Non-Cryst. Solids **32**, 207 (1979); T. Hamada and F. E. Fujita, Jpn. J. Appl. Phys. **24**, 249 (1985).
5. R. Ray and R. Hasegawa, Solid State Commun. **27**, 471 (1978).
6. F. H. Sánchez, J. I. Budnick, Y. D. Zhang, W. A. Hines, and M. Choi, Phys. Rev. B **34**, 4738 (1986).
7. J. I. Budnick, F. H. Sánchez, Y. D. Zhang, M. Choi, W. A. Hines, Z. Y. Zhang, S. H. Ge, and R. Hasegawa, IEEE Trans. Magn. MAG **23**, 1937 (1987).
8. M. B. Fernández van Raap and F. H. Sánchez, in *Applications of the Mössbauer Effects,* Proceedings of the First Latin American Conference, edited by E. Baggio-Saitovich, E. Galvao da

Silva, and H. R. Rechenbergs (World Scientific, Singapore, 1990), p. 278.
9. M. B. Fernández van Raap and F. H. Sánchez, J. Appl. Phys. **66**, 875 (1989).
10. R. Hasegawa and R. Ray, J. Appl. Phys. **49**, 4174 (1978).
11. J. I. Budnick and S. Sokalski, in *Hyperfine Interactions,* edited by A. J. Freeman and R. B. Frankel (Academic Press, New York, 1967), p. 724.
12. A. Vertés, L. Korecz, and K. Burgeer, in *Mössbauer Spectroscopy* (Elsevier Scientific Publishing Company, New York, 1979), p. 33.
13. J. Welfringer, Thesis, Lorraine (1983).
14. B. Leminus, These d'Etat Strasbourg (1978).
15. C. L. Chien, D. Musser, E. M. Gyorgy, R. C. Sherwood, H. S. Chen, F. E. Luborsky, and J. L. Walter, Phys. Rev. B **20**, 283 (1979).
16. L. Tackás, M. C. Cadeville, and I. Vincze, J. Phys. F5, 800 (1975).
17. Y. D. Zhang, J. I. Budnick, F. H. Sánchez, W. A. Hines, D. P. Yang, and J. D. Livingston, J. Appl. Phys. **61**, 4358 (1987).
18. M. Wojcik, H. Lerchner, P. Deppe, F. S. Li, M. Rosenberg, and J. D. Livingston, J. Appl. Phys. **55**, 2288 (1984).
19. F. H. Sánchez, M. B. Fernández van Raap, and J. I. Budnick, Phys. Rev. B **46**, 13881 (1992).
20. C. M. Brakman, A. W. J. Gommers, and E. J. Mittemeijer, J. Mater. Res. **4**, 1354 (1989).
21. R. Ingalls, F. van der Woude, and G. A. Sawatzky, in *Mössbauer Isomer Shifts,* edited by G. K. Shenoy and F. W. Wagner (North-Holland, Amsterdam, 1978), pp. 415–418.
22. R. Ingalls, Solid State Commun. **14**, 11 (1974).
23. F. H. Sánchez and M. B. Fernández van Raap, Phys. Rev. B **46**, 9013 (1992).
24. P. H. Gaskell, in *Glassy Metals II,* edited by H. Beck and H. J. Güntherodt (Springer-Verlag, Berlin-Heidelberg-New York, 1983), p. 16.
25. J. C. Ford, J. I. Budnick, W. A. Hines, and R. Hasegawa, J. Appl. Phys. **55** (6), 2286 (1984).
26. T. Shinjo, F. Itoh, H. Takaki, Y. Nakamura, and N. Shinkazono, J. Phys. Soc. Jpn. **19**, 1252 (1964).
27. G. Le Caër and J. M. Dubois, Phys. Status Solidi A **64**, 275 (1981).
28. W. K. Choo and R. Kaplow, Metall. Trans. **8A**, 417 (1977).
29. J. M. Dubois, These de Doctorat d' Etat, Nancy (1981).
30. H. Franke, U. Herold, U. Köster, and M. Rosenberg, in *Rapidly Quenched Metals III,* edited by B. Cantor (Chameleon, London, 1978), p. 155.
31. S. S. Hanna, J. Heberle, C. Littlejohn, G. Perlow, R. S. Preston, and D. H. Vincent, Phys. Rev. Lett. **4**, 177 (1960).
32. U. Gonser, C. J. Meechan, A. H. Muir, and H. Wiedersich, J. Appl. Phys. **34**, 2373 (1963).
33. K. A. Murphy and N. Hershkowitz, Phys. Rev. B **7**, 23 (1973).